

Modular Lipid Nanoparticle Platform Technology for siRNA and Lipophilic Prodrug Delivery

Roy van der Meel,* Sam Chen, Josh Zaifman, Jayesh A. Kulkarni, Xu Ran S. Zhang, Ying K. Tam, Marcel B. Bally, Raymond M. Schiffelers, Marco A. Ciufolini, Pieter R. Cullis, and Yuen Yi C. Tam

Successfully employing small interfering RNA (siRNA) therapeutics requires the use of nanotechnology for efficient intracellular delivery. Lipid nanoparticles (LNPs) have enabled the approval of various nucleic acid therapeutics. A major advantage of LNPs is the interchangeability of its building blocks and RNA payload, which allow it to be a highly modular system. In addition, drug derivatization approaches can be used to synthesize lipophilic small molecule prodrugs that stably incorporate in LNPs. This provides ample opportunities to develop combination therapies by co-encapsulating multiple therapeutic agents in a single formulation. Here, it is described how the modular LNP platform is applied for combined gene silencing and chemotherapy to induce additive anticancer effects. It is shown that various lipophilic taxane prodrug derivatives and siRNA against the androgen receptor, a prostate cancer driver, can be efficiently and stably co-encapsulated in LNPs without compromising physicochemical properties or gene-silencing ability. Moreover, it is demonstrated that the combination therapy induces additive therapeutic effects *in vitro*. Using a double-radiolabeling approach, the pharmacokinetic properties and biodistribution of LNPs and prodrugs following systemic administration in tumor-bearing mice are quantitatively determined. These results indicate that co-encapsulating siRNA and lipophilic prodrugs into LNPs is an attractive and straightforward plug-and-play approach for combination therapy development.


1. Introduction

Treating diseases by silencing pathological genes, expressing therapeutic proteins, or via gene editing is increasingly becoming a clinical reality. Several nucleic-acid-based therapeutics, such as antisense oligonucleotides, small interfering RNA (siRNA), messenger RNA (mRNA), and plasmid DNA, have been approved or are in late-stage clinical trials.^[1-5] As genetic drugs can modulate the expression of virtually any gene, they have the potential to therapeutically regulate targets considered “undruggable” by small molecule drugs. However, successfully employing nucleic acids as therapeutics depends heavily on chemical modifications and nanotechnology to prevent their degradation in the circulation and facilitate intracellular delivery.^[6,7]

The first siRNA therapeutic, Onpatro, was approved in 2018 for treatment of hereditary transthyretin-mediated amyloidosis,^[8,9] 20 years after the discovery

Dr. R. van der Meel, Prof. R. M. Schiffelers
Laboratory of Clinical Chemistry and Haematology
University Medical Center Utrecht
Utrecht 3584 CX, The Netherlands
E-mail: r.v.d.meel@tue.nl

Dr. R. van der Meel, Dr. S. Chen, Dr. J. A. Kulkarni, X. R. S. Zhang,
Prof. P. R. Cullis, Dr. Y. Y. C. Tam
Department of Biochemistry and Molecular Biology
University of British Columbia
Vancouver, BC V6T 1Z3, Canada

 The ORCID identification number(s) for the author(s) of this article can be found under <https://doi.org/10.1002/smll.202103025>.

© 2021 The Authors. Small published by Wiley-VCH GmbH. This is an open access article under the terms of the Creative Commons Attribution-NonCommercial-NoDerivs License, which permits use and distribution in any medium, provided the original work is properly cited, the use is non-commercial and no modifications or adaptations are made.

DOI: 10.1002/smll.202103025

Dr. R. van der Meel
Laboratory of Chemical Biology
Department of Biomedical Engineering and Institute
for Complex Molecular Systems
Eindhoven University of Technology
P.O. Box 513, 5600 MB, Eindhoven, The Netherlands

Dr. S. Chen, Dr. J. Zaifman, Dr. Y. Y. C. Tam
Integrated Nanotherapeutics
Burnaby, BC V5G 4X4, Canada

Dr. J. Zaifman, Prof. M. A. Ciufolini
Department of Chemistry
University of British Columbia
Vancouver, BC V6T 1Z1, Canada

Dr. J. A. Kulkarni
Department of Medical Genetics
University of British Columbia
Vancouver, BC V6H 3N1, Canada

Dr. Y. K. Tam
Acuitas Therapeutics
Vancouver, BC V6T 1Z3, Canada

of RNA interference.^[10] Onpatro relies on lipid nanoparticle (LNP) technology for siRNA delivery to hepatocytes, where it inhibits production of the disease-causing mutant transthyretin protein.^[11] Most recently, LNP technology has also enabled the rapid development and (emergency) approval of mRNA-based vaccines against COVID-19.^[12,13] LNPs are generally $\approx 50\text{--}80$ nm in diameter, depending on the nucleic acid payload, and consist of cholesterol, phospholipids, polyethylene glycol-conjugated lipids, and ionizable cationic lipids. Ionizable amino lipids with an apparent pK_a of around 6.4 are a key component, as their use enables efficient siRNA encapsulation during LNP production at low pH (≤ 4), ensures a neutral surface charge of the LNPs in the circulation at physiological pH, and promotes endosomal escape following target cell internalization.^[14,15]

The major advantage of LNP technology is its modularity, which readily enables the rapid development of siRNA and other nucleic acid therapeutics. The siRNA payload is interchangeable as its physicochemical properties remain similar regardless of its sequence. As such, in addition to siRNA drugs for hepatic^[16] and extrahepatic^[17,18] targets, LNP technology has also been employed for the therapeutic application of mRNA^[19–22] and gene editing.^[23] Moreover, the modular design space of LNPs can be expanded by drug derivatization approaches whereby small molecule prodrugs can be synthesized and stably incorporated in LNPs. Incorporating such prodrugs in nanocarriers reduces the differences in physicochemical characteristics, pharmacokinetic properties, and biodistribution profiles among various drug molecules, thereby improving drug encapsulation predictability.^[24] In addition, these approaches can reduce drug-induced systemic toxicity and improve therapeutic efficacy.^[25,26] Finally, modular prodrug designs provide opportunities to co-encapsulate multiple therapeutic agents in a single nanocarrier.

We have recently developed a prodrug platform technology for efficiently incorporating small molecule therapeutics in LNPs.^[27,28] The rationally designed prodrugs consist of an active drug coupled via a biodegradable (ester) linker to a hydrophobic moiety. Following cellular uptake of LNPs, intracellular enzymes break down the linker, releasing the active drug. Using this approach, we demonstrated that incorporating prodrug derivatives of the corticosteroid dexamethasone

in LNP formulations containing nucleic acids significantly reduced their immunostimulatory effects following parenteral administration.^[27]

Here, we demonstrate that the modular LNP platform can be used for combined gene silencing and chemotherapy to induce additive anticancer effects. As a proof of concept, we co-encapsulated siRNA against the N-terminal domain of the androgen receptor (AR), a prostate cancer driver, and various lipophilic prodrug derivatives of the chemotherapeutic agents, docetaxel (DTX) and cabazitaxel (CBZ). We show that taxane prodrugs can be stably incorporated in LNP–siRNA systems, which prodrug incorporation does not affect the formulation's ability to knockdown the AR target gene and that the combination formulation induces additive therapeutic effects *in vitro*. In addition, we used a double-radiolabeling approach to quantitatively determine the pharmacokinetic properties and biodistribution of the LNPs and prodrugs following systemic administration. Finally, we show prodrug accumulation and significant AR target gene knockdown in tumors following systemic LNP administration in a murine xenograft tumor model.

2. Results and Discussion

2.1. Formulating and Analyzing Lipid Nanoparticles Containing siRNA and Taxane Prodrugs

The utility of lipophilic prodrugs in LNP–siRNA systems has to meet several requirements.^[29,30] First, prodrug incorporation must not disrupt LNP formation and siRNA entrapment during the formulation process. Second, it should not significantly alter LNP stability or its physicochemical parameters. Third, the prodrug and siRNA payloads have to maintain their therapeutic activity. To investigate which taxane prodrug is best suited for LNP incorporation, we synthesized two lipophilic docetaxel derivatives (LD18 and LD22) and two cabazitaxel derivatives (LD27 and LD28) by conjugating various hydrocarbon chains to the taxane C2'-hydroxyl groups through the use of biodegradable ester linkages (**Figure 1**).

The synthesized lipophilic taxane prodrugs and siRNA were incorporated in LNPs by a rapid mixing procedure using a T-junction device as previously described.^[14,27,31,32] The lipid compositions, based on the optimized LNP formulation used for Onpatro,^[11,15] are listed in Table S1 (Supporting Information).

As shown in **Table 1**, LNP–siRNA formulations containing 1 mol% docetaxel prodrugs LD18 or LD22 (for *in vitro* studies) had particle diameters of ≈ 50 nm by Z-average, with polydispersity indices (PDI) ≤ 0.1 and nearly neutral zeta potentials. LNP formulations containing 1 mol% cabazitaxel prodrugs LD27 or LD28 had comparable physicochemical characteristics (Table S2, Supporting Information). Moreover, LNP formulations containing 10 mol% LD18 or LD22 (for *in vitro* and *in vivo* studies) (Tables S3–5, Supporting Information) had similar properties compared to formulations containing 1 mol% prodrug, indicating that prodrug incorporation up to 10 mol% did not significantly affect LNP size, homogeneity, or zeta potential. These results were corroborated by cryogenic transmission electron microscopy (cryoTEM), which demonstrated that LNPs containing 10 mol% LD18 or LD22 displayed similar

Prof. M. B. Bally
Experimental Therapeutics
BC Cancer Research Centre
Vancouver, BC V5Z 1L3, Canada

Prof. M. B. Bally
Department of Pathology and Laboratory Medicine
University of British Columbia
Vancouver, BC V6T 1Z7, Canada

Prof. M. B. Bally
Faculty of Pharmaceutical Sciences
University of British Columbia
Vancouver, BC V6T 1Z3, Canada

Prof. M. B. Bally
Centre for Drug Research and Development
Vancouver, BC V6T 1Z3, Canada

Prof. P. R. Cullis
NanoMedicines Innovation Network
University of British Columbia
Vancouver, BC V6T 1Z3, Canada

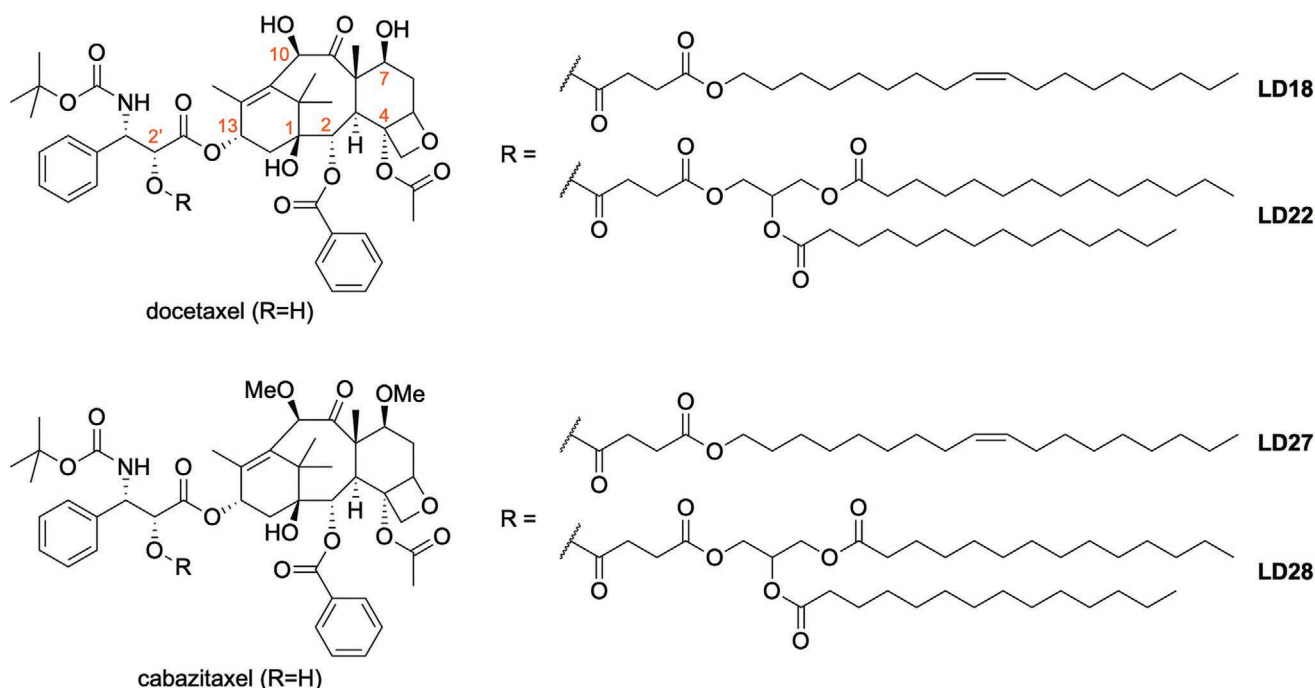


Figure 1. Lipophilic docetaxel and cabazitaxel prodrugs with varying hydrophobic moieties.

morphology and size when compared to control formulations without prodrugs (Figure 2). Efficient prodrug and siRNA entrapment (routinely >90%) were observed for all formulations containing 0.1–10 mol% taxane prodrugs.

The cytotoxic activity of the taxane prodrugs is dependent upon the release of the prodrugs from the LNP–siRNA systems and the subsequent esterase-mediated liberation of the active compounds (Figure S2, Supporting Information). To assess activity, LNP–siRNA containing 10 mol% docetaxel prodrugs LD18 and LD22 were incubated with esterase-rich mouse plasma, and the amount of parent prodrug remaining was determined. After 24 h incubation, ≈75% and ≈50% of LNP-associated LD18 and LD22, respectively, were degraded (Figure 3A). The variation in degradation could be caused by differences in prodrug lipophilicity and LNP incorporation. It is possible that the more lipophilic LD22, which contains two saturated C₁₄ lipid chains, incorporates more stably in the hydrophobic LNP core

during production and is therefore less accessible to esterases. Similar results have been observed when lipophilic dexamethasone prodrugs were incorporated in LNP–siRNA.^[27]

To determine if the liberated taxane compounds maintain their functionality and induce cytotoxicity, prodrugs were first incubated with mouse plasma followed by exposure to prostate cancer cells. As shown in Figure 3B, taxane prodrugs significantly reduced 22Rv1 cell viability following mouse plasma preincubation when compared to prodrugs preincubated in regular culture medium. This was not observed for unmodified docetaxel and cabazitaxel, which were equally potent regardless of culture medium or mouse plasma preincubation. Similar results were observed with PC3 cells (Figure S3, Supporting Information). This indicates that derivatizing taxane chemotherapeutics for stable LNP incorporation likely reduces their toxicity, but cytotoxic activity is again restored when the active compound is liberated in an esterase-rich environment.

Table 1. Physicochemical analysis of lipid nanoparticles used for in vitro studies. Data are presented as mean ± standard deviation (SD) of three representative formulation batches. LNP, lipid nanoparticle; LD, lipophilic prodrug; LDE, laser Doppler electrophoresis; PDI, polydispersity index; TL, total lipid; wt, weight.

LD	siRNA	Dynamic light scattering (DLS)			Ribogreen assay	UPLC	Cholesterol assay		LDE
		Z-average [nm]	Mean number [nm]	PDI	siRNA:lipid ratio [wt:wt]	LD:lipid ratio [wt:wt]	TL [mg mL ⁻¹]	TL [× 10 ⁻³ M]	Zeta potential [mV]
–	Luc	50 ± 0.4	38 ± 0.5	0.07 ± 0.005	0.036 ± 0.006	–	5.6 ± 0.6	9.7 ± 1.1	0.41 ± 7.19
	ARNTD	50 ± 0.6	37 ± 0.2	0.07 ± 0.002	0.035 ± 0.004	–	6.4 ± 0.6	10.9 ± 1.0	–2.00 ± 8.53
1 mol% LD18	Luc	53 ± 3.8	38 ± 1.5	0.10 ± 0.016	0.032 ± 0.002	0.014 ± 0.001	5.8 ± 0.5	9.9 ± 0.9	–1.99 ± 6.60
	ARNTD	51 ± 1	39 ± 1.4	0.06 ± 0.007	0.034 ± 0.005	0.013 ± 0.002	6.4 ± 0.8	11 ± 1.4	–1.81 ± 5.92
1 mol% LD22	Luc	53 ± 0.01	38 ± 0.5	0.09 ± 0.006	0.034 ± 0.001	0.014 ± 0.001	6.3 ± 0.4	10.7 ± 0.6	–1.67 ± 6.98
	ARNTD	52 ± 1.6	39 ± 0.6	0.06 ± 0.009	0.033 ± 0.003	0.013 ± 0.001	6.60 ± 0.6	11.3 ± 1.0	–1.89 ± 5.87

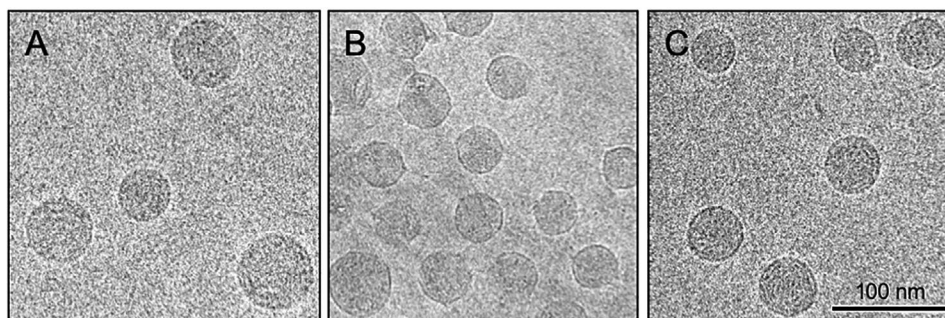


Figure 2. Cryogenic transmission electron microscopic images of lipid nanoparticles containing siRNA and lipophilic docetaxel prodrugs. Lipid nanoparticles containing A) luciferase siRNA alone, B,C) luciferase siRNA and 10 mol% docetaxel prodrugs B) LD18 or C) LD22 were visualized using cryogenic transmission electron microscopy operating at 200 kV.

2.2. LNPs Containing Androgen Receptor siRNA and Taxane Prodrugs Induce Additive Therapeutic Effects In Vitro

We next assessed the therapeutic efficacy of LNPs in vitro by determining their ability to induce target gene knockdown and inhibit cell viability using various genetically distinct prostate cancer cell lines. In 22Rv1 cells, which express wild-type AR and the frequently occurring splice variant, AR variant 7 (AR-V7), LNPs containing siRNA against AR N-terminal domain (ARNTD) significantly silenced AR-V7 expression at doses as low as $0.01 \mu\text{g mL}^{-1}$ siRNA when compared to control LNP formulations containing luciferase siRNA (Figure S4A–C, Supporting Information). To evaluate if taxane prodrug incorporation affects the gene knockdown activity of LNP–siRNA, we incubated 22Rv1 and LNCaP cells with LNPs containing 1 mol% taxane prodrugs and ARNTD siRNA, and measured the resulting AR-V7 expression levels.

As shown in Figure 4A,B, LNPs containing ARNTD siRNA and docetaxel or cabazitaxel prodrugs induced significant

AR-V7 knockdown when compared to control formulations containing prodrugs and luciferase siRNA at a dose of $0.05 \mu\text{g mL}^{-1}$ siRNA. Similar effects were observed when 22Rv1 cells were exposed to LNPs in medium containing charcoal-stripped serum and synthetic androgen, an environment that mimics castration-resistant prostate cancer conditions (Figure S6, Supporting Information). These results show that prodrug incorporation does not affect the gene-silencing ability of LNP–siRNA. Of note, in 22Rv1 cells a reduction of AR-V7 expression was observed after treatment with LNPs containing siRNA against firefly luciferase (siLuc) and docetaxel prodrugs (Figure 4A). This nonspecific gene-silencing effect is possibly due to the cytotoxic mechanism of action of docetaxel. It has previously been reported that microtubule disruption by docetaxel can have an effect on AR-V7 gene expression.^[33]

We next determined the effect of silencing AR or AR-V7 on cell viability. Exposing 22Rv1 cells for 96 h to LNPs containing ARNTD siRNA at a dose of $0.05 \mu\text{g mL}^{-1}$ siRNA resulted in significant cytotoxicity, while no decrease in cell viability was

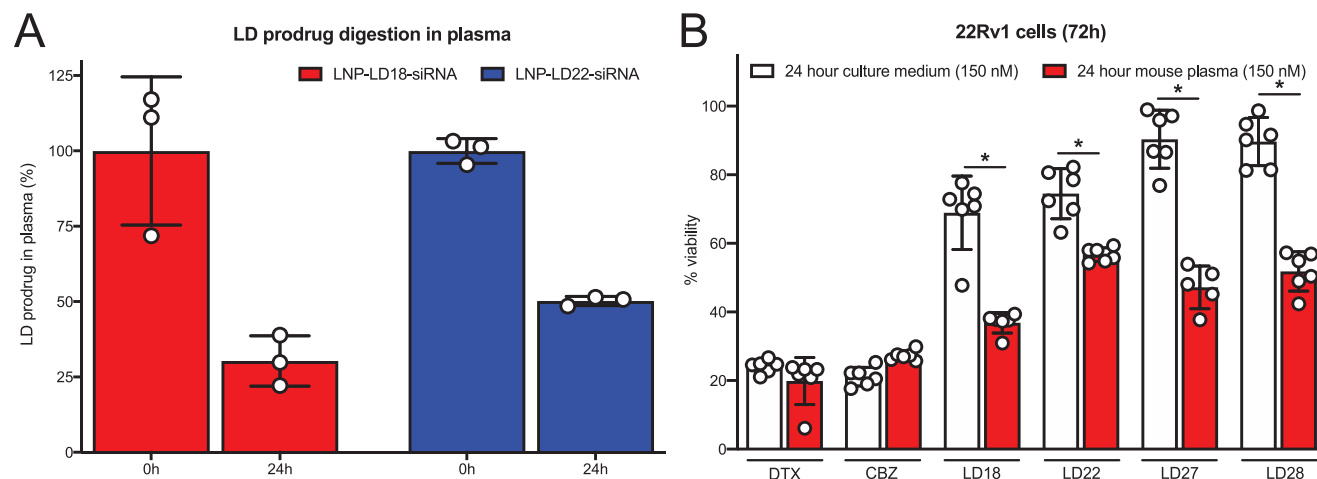


Figure 3. Esterase-mediated hydrolytic activation of lipophilic taxane prodrugs. A) Docetaxel prodrug digestion in plasma. LNPs containing luciferase siRNA and 10 mol% docetaxel prodrug LD18 or LD22 were incubated with CD1 mouse plasma for 24 h. Prodrug concentration in plasma samples was determined by UPLC analysis. Reduction in parent prodrug amount indicates digestion in plasma. Data represent mean \pm standard deviation (SD; $n = 3$) of one representative experiment. B) Incubating taxane prodrugs with murine plasma liberates active cytotoxic parent compounds. Docetaxel (DTX) prodrugs (LD10, LD18, LD22, and LD23) and cabazitaxel (CBZ) prodrugs (LD27 and LD28) were incubated in culture medium or CD1 mouse plasma at 37°C for 24 h prior to 72 h 22Rv1 cell treatment. Cytotoxicity was determined by MTS cell viability assay. Data are presented as mean \pm SD of one representative experiment ($n = 6$) and analyzed by two-way analysis of variance (ANOVA) with Tukey's posthoc test. * indicates the p -value of <0.005 plasma incubation versus culture medium incubation.

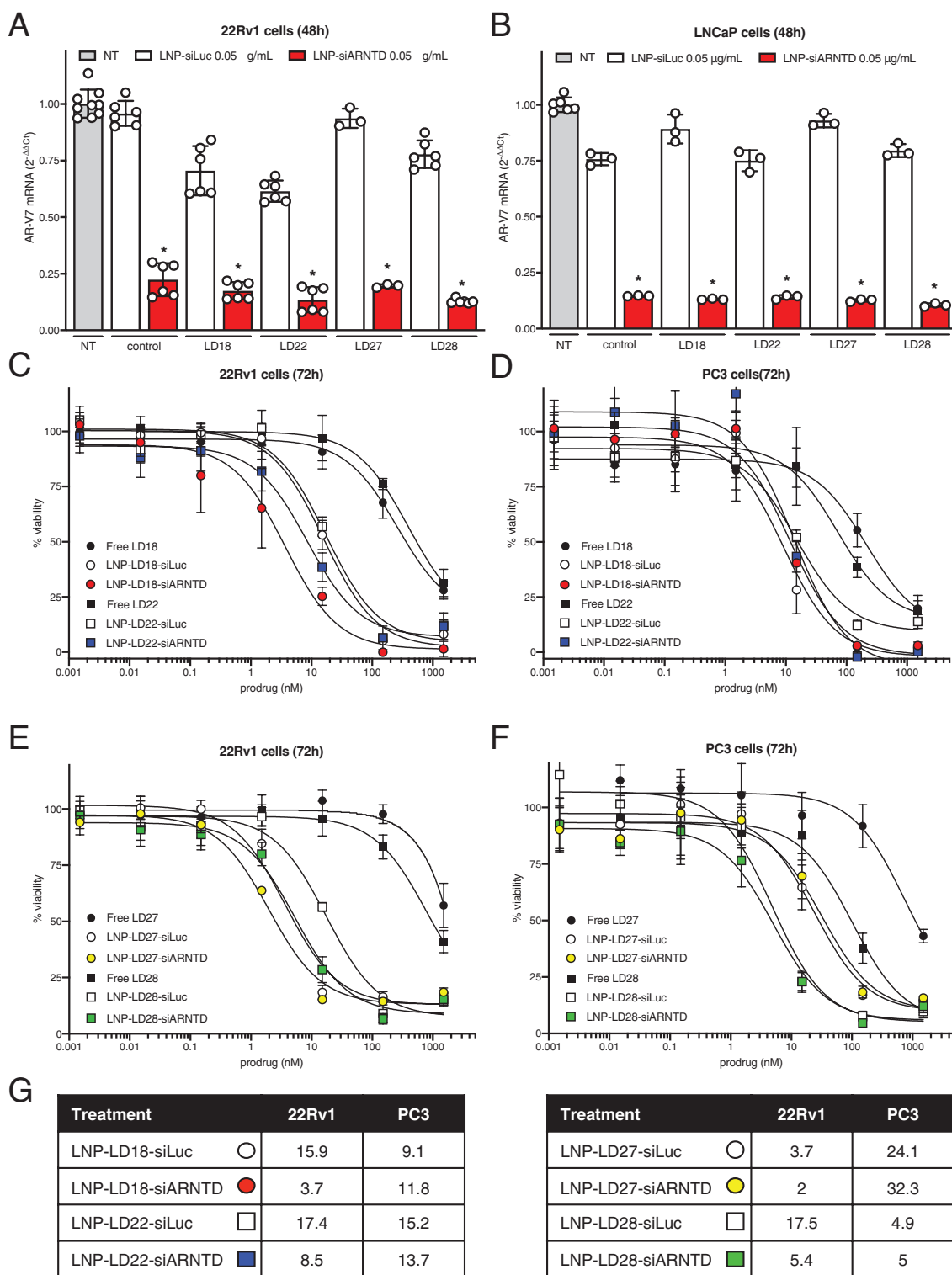


Figure 4. Lipid nanoparticles containing taxane prodrugs and androgen receptor siRNA induce target gene knockdown and inhibit cell viability. A) 22Rv1 and B) LNCaP cells were exposed for 48 h to LNPs containing 1 mol% docetaxel (LD18 and LD22) or cabazitaxel (LD27 and LD28) prodrugs and siRNA against luciferase (siLuc) or androgen receptor (AR) N-terminal domain (siARNTD) at a dose of 0.05 $\mu\text{g mL}^{-1}$. LNP-siRNA without incorporated prodrugs were used as control. RT-qPCR was used to determine mRNA levels. AR variant 7 (AR-V7) target gene expression change was calculated relative to β -actin control. Data represent mean \pm SD ($n = 3$) of one or two representative experiments and analyzed by one-way ANOVA with Tukey's posthoc test. * indicates the p -value of <0.0001 of LNP formulations containing siARNTD versus siLuc control. C, E) 22Rv1 and D, F) PC3 cells were exposed for 72 h to LNPs containing 1 mol% taxane prodrugs and siLuc or siARNTD. Cell viability was determined by MTS assay. Data are presented as mean \pm SD of one representative experiment ($n = 6$). G) IC_{50} values ($\times 10^{-9}$ M prodrug) derived from data in panels (C)–(F) determined by Graphpad Prism 8.

observed for LNPs containing luciferase siRNA (Figure S4D, Supporting Information). Importantly, exposing PC3 cells, which do not express AR or AR-V7, to the same siRNA dose did not result in cell viability inhibition for LNPs containing either ARNTD or luciferase siRNA (Figure S4D, Supporting Information). This indicates that the cell viability inhibition is a result of specific AR/AR-V7 knockdown induced by LNPs containing ARNTD siRNA.

To determine if AR/AR-V7 knockdown and taxane-induced cytotoxicity would induce additive therapeutic effects, we first exposed prostate cancer cells to increasing concentrations of docetaxel or cabazitaxel combined with LNPs containing ARNTD siRNA at a constant dose of $0.05 \mu\text{g mL}^{-1}$. As shown in Figure S5 (Supporting Information), additive cytotoxic effects were observed in AR/AR-V7-expressing 22Rv1 and VCaP cells, but not PC3 cells. Encouraged by these results, we proceeded to expose 22Rv1 and PC3 cells to increasing concentrations of LNPs containing 1 mol% lipophilic taxane prodrugs and ARNTD siRNA (Figure 4). In both cell lines, LNPs containing taxane prodrugs and ARNTD or luciferase siRNA induced dose-dependent cell viability inhibition. However, in 22Rv1 cells, LNPs with ARNTD siRNA were considerably more potent than control formulations containing luciferase siRNA. For example, the half-maximal inhibitory concentration (IC_{50}) value of LNPs containing ARNTD and docetaxel prodrug LD18 was $3.7 \times 10^{-9} \text{ M}$ (prodrug concentration), while the IC_{50} value was $15.9 \times 10^{-9} \text{ M}$ for the control formulation. For formulations containing docetaxel prodrug LD22, these values were $8.5 \times 10^{-9} \text{ M}$ for the LNPs containing ARNTD siRNA versus $174 \times 10^{-9} \text{ M}$ for the control formulation (Figure 4C,G). In contrast, in PC3 cells, the IC_{50} values were comparable for LNPs containing taxane prodrugs and ARNTD or luciferase siRNA (Figure 4D,G) as PC3 cells do not express AR or AR-V7. Similar results were observed for formulations containing cabazitaxel prodrugs (Figure 4E,F) and LNPs containing 0.1 mol% taxane prodrugs (Figure S7, Supporting Information). Of note, the activity of free docetaxel and cabazitaxel prodrugs in both cell lines is limited, while prodrug incorporation in LNPs containing luciferase siRNA results in dose-dependent cell viability inhibition. This indicates that taxane prodrug derivatization impairs their cell uptake, and encapsulation in LNP is required for intracellular access and subsequent antiproliferation effect.

2.3. Taxane Prodrugs Remain Associated with Lipid Nanoparticles Following Systemic Administration

It has previously been shown that LNP-siRNA can accumulate in tumors and induce therapeutic effects following systemic administration in prostate cancer xenograft mouse models.^[18,34,35] The tumor accumulation of LNPs largely depends on the ability of LNPs to stay intact and circulate for a sufficient length of time in order to accumulate in the tumor microenvironment. To determine if taxane prodrug incorporation affects LNP circulation time, we formulated ^{14}C -radiolabeled LNP-siRNA containing ^3H -labeled taxane prodrugs and conducted pharmacokinetic studies in CD1 mice following systemic administration. This double radiolabeling approach allowed us to quantitatively track both the LNP and the taxane prodrug payload by gamma counting, making it

possible to determine if the prodrug remains associated with the LNP over time following intravenous injection.

We first determined the circulation time of control LNP-siRNA by using ^{14}C -labeled 1,2-distearoyl-*sn*-glycero-3-phosphorylcholine (DSPC) and ^3H -labeled cholesteryl hexadecyl ether (CHE) in the formulation. As shown in Figure 5A, the percentage of injected dose quantification at various time points provided identical outcomes when determined by ^{14}C -labeled DSPC ($T_{1/2} = 4.63 \text{ h}$) or ^3H -CHE ($T_{1/2} = 4.55 \text{ h}$). In addition, other LNP-siRNA pharmacokinetic parameters such as distribution volume, clearance, and area under the curve (AUC^∞) were also comparable for both radiolabels (Figure 5E). These results demonstrate that the incorporation of ^{14}C -labeled DSPC in LNPs combined with ^3H -labeled prodrugs represents a reliable strategy to determine the pharmacokinetic parameters of both the nanocarrier and the prodrug payload following systemic administration to mice.

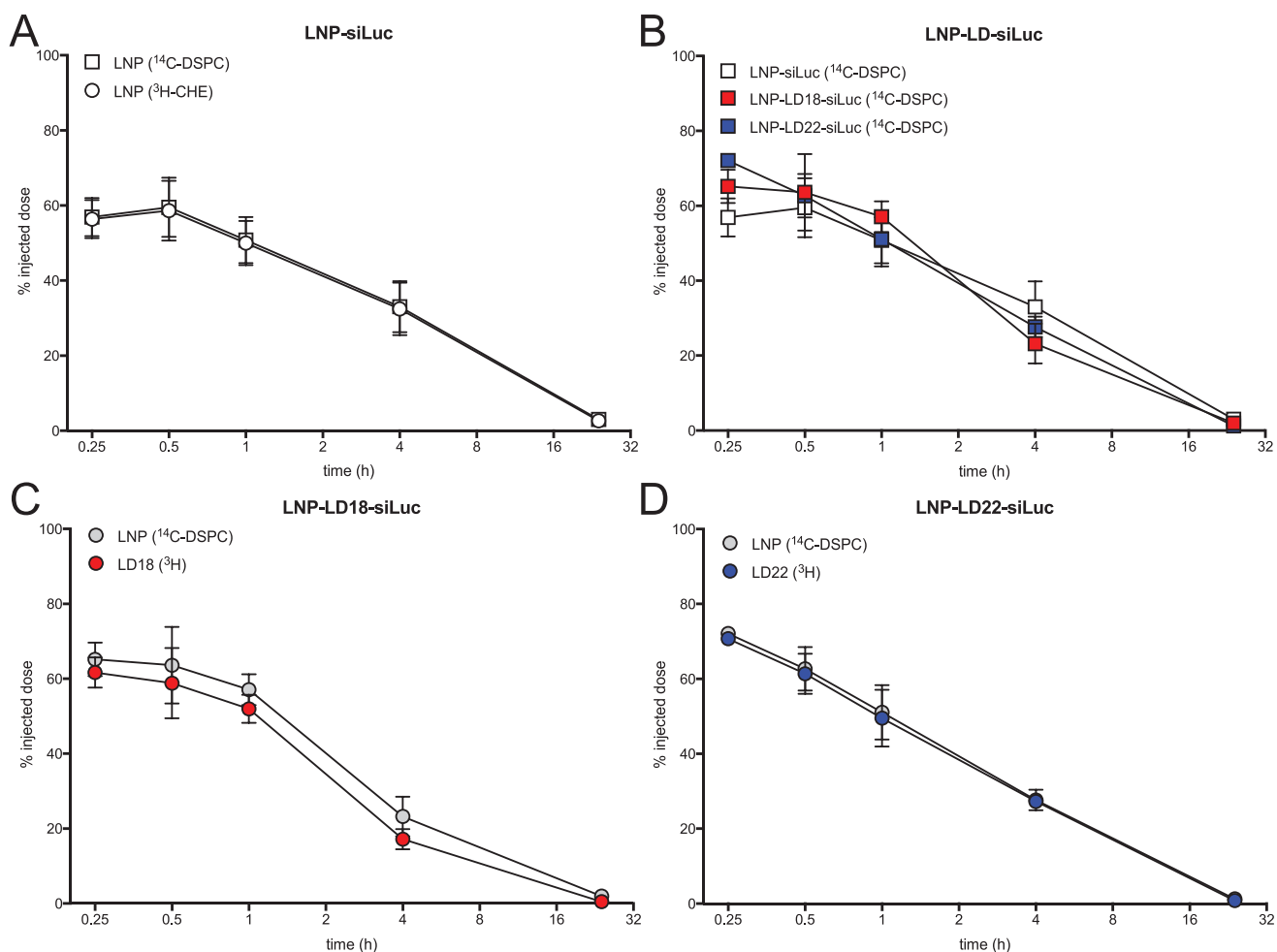
Although control LNP-siRNA and formulations containing LD18 or LD22 prodrugs showed comparable pharmacokinetic profiles as determined by ^{14}C -DSPC (Figure 5B), prodrug incorporation appears to affect LNP circulation time to some extent. The $T_{1/2}$ of 2.6 h for LNPs containing prodrugs was slightly shorter than that of control LNP-siRNA. In line with this, LNPs containing prodrugs had a slightly faster clearance and lower AUC^∞ compared to control formulations (Figure 5E). This may be attributed to the lower cholesterol and phospholipid amount present in the formulation containing prodrugs compared to control formulations (Table S1, Supporting Information), which could affect the opsonization and subsequent blood clearance of the LNPs.^[36]

Importantly, the circulation time of the ^3H -labeled LD18 ($T_{1/2} = 2.11 \text{ h}$) and LD22 ($T_{1/2} = 2.65 \text{ h}$) prodrugs was comparable to that of their respective LNP-siRNA formulation (Figure 5C,D), indicating that the prodrugs remain associated with the LNPs in the circulation. This suggests that LNPs have the potential to simultaneously deliver their siRNA and prodrug payload to target cells following systemic administration, which is important for their therapeutic effect.

2.4. Lipid Nanoparticles Deliver siRNA and Taxane Prodrugs to Tumors

To determine to what extent LNP-siRNA and associated taxane prodrugs accumulate in tumors following systemic administration, we conducted a biodistribution study using a 22Rv1 subcutaneous tumor xenograft model in mice. As with the pharmacokinetic study, ^{14}C -radiolabeled LNP-siRNA containing ^3H -labeled prodrugs were used to determine the individual tissue biodistribution of both the LNPs and the prodrug payload.

Figure 6A–C shows the tissue distribution of the control formulation and LNP-siRNA containing docetaxel prodrugs LD18 or LD22, 24 h following intravenous injection. Despite differences in pharmacokinetic parameters, unmodified and prodrug-containing LNPs showed comparable tissue distribution. The highest LNP accumulation was observed in the liver ($\pm 15\%$ injected dose per gram tissue, ID g^{-1} tissue). This is expected as LNPs are known to be efficiently taken up by hepatocytes.^[14,15] LNP accumulation was also observed in the spleen



E

Treatment		$T_{1/2}$ (h)	V_D ((ID)/(%ID))	CL ((ID)/(%ID)/h)	AUC_0^t (%ID*h)	AUC_0^∞ (%ID*h)
LNP-siLuc (¹⁴ C-DSPC)	□	4.63	1.65	0.25	394.24	405.37
LNP-siLuc (³ H-CHE)	○	4.55	1.67	0.25	383.75	393.92
LNP-LD18-siLuc (¹⁴ C-DSPC)	■	2.56	1.39	0.38	265.64	266.05
LNP-LD22-siLuc (¹⁴ C-DSPC)	■	2.64	1.38	0.36	276.03	276.54
LD18 (³ H)	●	2.11	1.45	0.48	209.66	209.74
LD22 (³ H)	●	2.65	1.41	0.37	270.65	271.16

Figure 5. Pharmacokinetic parameters of double-radiolabeled lipid nanoparticles following systemic administration in mice. LNP-siRNA containing 10 mol% docetaxel prodrug LD18 or LD22 had a double radiolabel to track both the LNP and the prodrugs in the circulation after injection. CD1 mice were injected intravenously with LNPs at a dose of 4 mg kg⁻¹ siRNA, corresponding to ±30 mg kg⁻¹ docetaxel prodrug. Blood samples were collected via cardiac puncture at various time points, and radiolabels were quantified by liquid scintillation counting. A) Circulation time of control LNPs containing siLuc determined by ³H-CHE and ¹⁴C-DSPC. B) Comparison of LNP circulation times as determined by ¹⁴C-DSPC. C) Circulation time of LNP-LD18-siLuc determined by ¹⁴C-DSPC (LNP) and ³H-LD18 (prodrug). D) Circulation time of LNP-LD22-siLuc determined by ¹⁴C-DSPC (LNP) and ³H-LD22 (prodrug). Data are presented as mean ± SD of one experiment (n = 3–4 animals per time point). E) Pharmacokinetic parameters of LNP formulations determined by PKSolver. $T_{1/2}$, elimination half-life; V_D , volume of distribution; CL, clearance; AUC, area under the curve.

(±4–5% ID g⁻¹ tissue), likely due to uptake by phagocytic cells. LNP accumulated to a comparable degree in the kidneys and to a lesser extent in the lungs and heart.

Importantly, for all LNP formulations, ≈2% ID g⁻¹ tissue accumulated in the tumor (Figure 6D). This is in line with the accumulation of other nanocarriers in solid tumors.^[37]

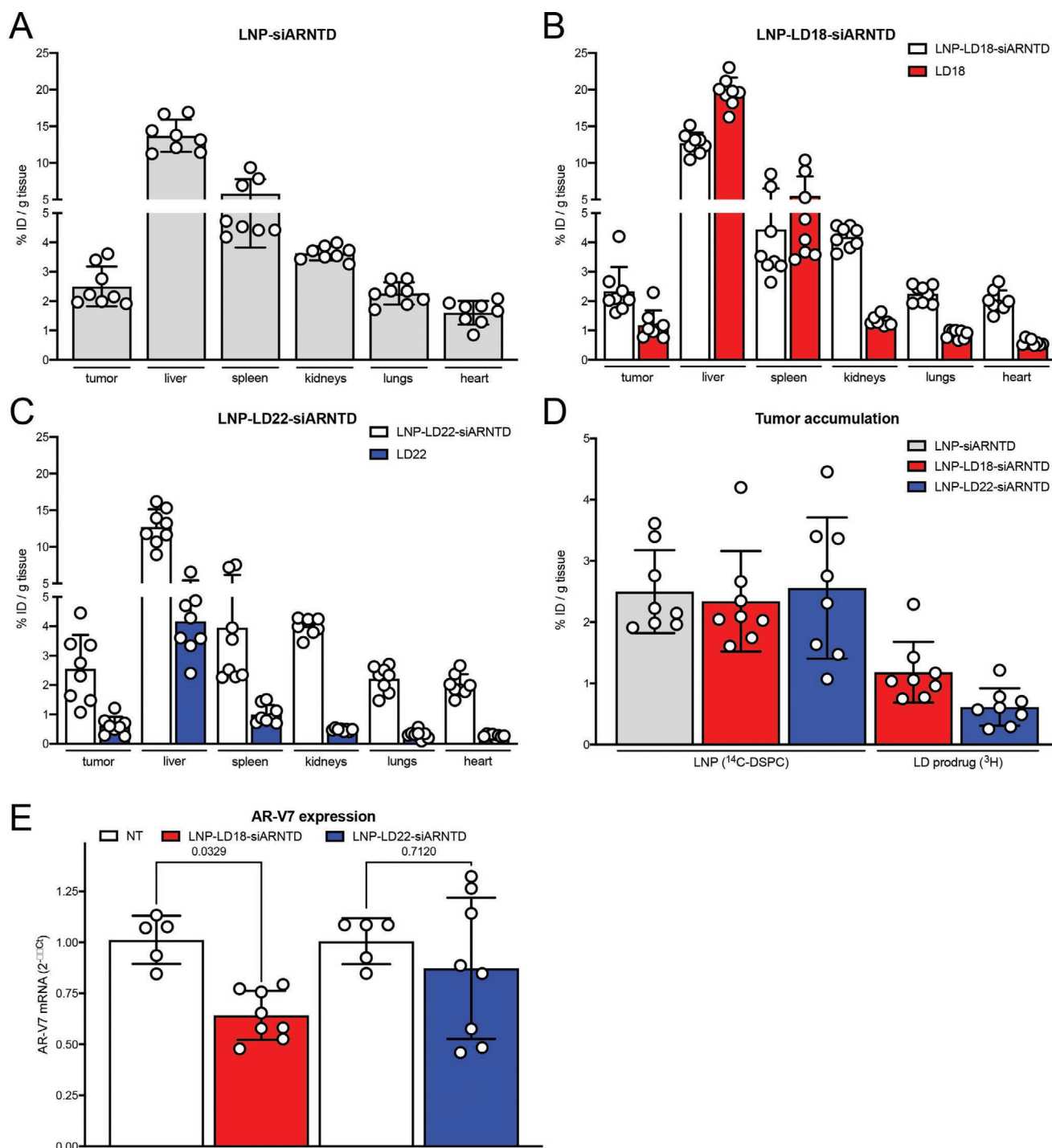


Figure 6. Lipid nanoparticles accumulate in tumors and induce target gene knockdown following systemic administration in mice. NRG mice bearing 22Rv1 tumors were injected intravenously with ^{14}C -DSPC-labeled LNP-siRNA containing 10 mol% ^3H -labeled docetaxel prodrug LD18 or LD22 at a dose of 5 mg kg^{-1} siRNA, corresponding to $\pm 30\text{ mg kg}^{-1}$ docetaxel prodrug. After 24 h, mice were sacrificed, and tissues were collected for radiolabel quantification by liquid scintillation counting. Tissue distribution profiles of A) control LNPs containing ARNTD siRNA (LNP-siARNTD), B) LNPs containing siARNTD and LD18 (LNP-LD18-siARNTD), and C) LNPs containing siARNTD and LD22 (LNP-LD22-siARNTD). D) Tumor accumulation of LNP formulations. Radioactivity is expressed as percent injected dose per gram ($\% \text{ID g}^{-1}$) of tissue. Data represent mean \pm SD ($n = 8$ animals). E) RT-qPCR was used to determine tumor mRNA levels. AR variant 7 (AR-V7) target gene expression change was calculated relative to β -actin control. Data represent mean \pm SD ($n = 8$ animals) of one experiment and analyzed by one-way ANOVA with Tukey's posthoc test.

Notable differences were observed in the tissue distribution of LD18 and LD22 (Figure 6B,C). For example, LD18 accumulated in the liver ($\pm 20\%$ ID g^{-1} tissue) and spleen ($\pm 5\%$ ID g^{-1} tissue), even to a higher extent than the associated LNP. In contrast, both the liver ($\pm 4\%$ ID g^{-1} tissue) and spleen ($\pm 1\%$ ID g^{-1} tissue) accumulation of LD22 were considerably lower. As shown in Figure 6D, the overall higher tissue accumulation of LD18 compared to LD22 was also observed in the tumor ($\pm 1.2\%$ vs 0.8% ID g^{-1} tissue, respectively). The cause of these differences in prodrug tissue accumulation remains unclear, since the associated LNP accumulation was comparable. Additional experiments with LNPs containing other taxane prodrug derivatives are required to determine how the structure and lipophilicity influence tissue accumulation.

Unmodified LNP–siRNA have previously been shown to be capable of inducing gene silencing in prostate cancer xenograft models.^[34,35] To determine if LNPs containing taxane prodrugs and ARNTD siRNA could induce AR-V7 knockdown, RNA was extracted from tumors collected during the biodistribution study and analyzed by quantitative reverse transcription polymerase chain reaction (qPCR) (Figure 6E). As expected, control LNP containing ARNTD siRNA (Figure S8, Supporting Information) and formulations containing ARNTD siRNA and LD18 significantly reduced AR-V7 levels compared to nontreated controls.

However, LNP containing LD22 did not induce significant AR-V7 knockdown even though LNP accumulation in tumors was similar to the other formulations. Although significant AR-V7 knockdown was induced in the tumors of three animals, considerable variation in gene silencing was observed in this treatment group. It is possible that this variation is caused by the low siRNA dosage used in this study (5 mg kg^{-1}). We have previously shown that repeated injections of 10 mg kg^{-1} were necessary to achieve $>70\%$ gene silencing. However, despite the lower siRNA dose (5 mg kg^{-1}) used in this study, control and LD18 LNP containing ARNTD siRNA significantly reduced AR-V7 levels compared to control animals.

Collectively, these results indicate that LNP–siRNA containing lipophilic taxane prodrugs are able to deliver their therapeutic payloads to tumors, resulting in target gene knockdown.

3. Conclusions

LNP nanocarrier technology has enabled the clinical translation of RNA-based gene therapies. At the same time, the modularity of LNPs and drug derivatization methods provide opportunities to develop rational combination strategies. For example, incorporating dexamethasone prodrugs to reduce the immunostimulatory properties of LNPs containing nucleic acids.^[27]

Here, we show that incorporating taxane prodrugs in LNP–siRNA systems offers an attractive strategy to induce additive anticancer effects via combined gene silencing and chemotherapy. Various lipophilic docetaxel and cabazitaxel derivatives were stably incorporated in LNPs without affecting its physicochemical properties or compromising the gene-silencing ability of LNP–siRNA. As a proof of concept, combined LNP–siRNA-mediated knockdown of AR, a prostate cancer driver, and taxane prodrug-induced cytotoxicity induced additive therapeutic effects in vitro. Finally, we demonstrated that prodrugs remain associated with LNP–siRNA following systemic administration,

resulting in prodrug accumulation and target gene knockdown in tumors in vivo. Our study indicates that co-encapsulation of siRNA and lipophilic prodrugs into LNPs provides opportunities for rational design of combination therapies.

4. Experimental Section

Materials: DSPC was purchased from Avanti Polar Lipids (Alabaster, AL) and cholesterol was obtained from Sigma–Aldrich (St. Louis, MO). DTX and CBZ were obtained from eNovation Chemicals (Bridgewater, NJ). ^3H -docetaxel was obtained from Moravec, Inc. (Brea, CA). The ionizable cationic lipid (6Z,9Z,28Z,31Z)-heptatriaconta-6,9,28,31-tetraen-19-yl-4-(dimethylamino) butanoate (DLin-MC3-DMA) was synthesized as previously described by Jayaraman et al.,^[15] while (R)-2,3-bis(tetradecyloxy)propyl-1-(methoxy polyethylene glycol 2000) carbamate (PEG-DMG) and (R)-2,3-bis(stearoyloxy)propyl-1-(methoxy polyethylene glycol 2000) carbamate (PEG-DSG) were synthesized as previously reported by Akinc et al.^[38] All lipid structures that were used in this study are shown in Figure S1 (Supporting Information).

Taxane Lipophilic Prodrug Synthesis: Docetaxel and cabazitaxel lipophilic prodrug synthesis are detailed in the Supporting Information.

Small Interfering RNA: All modified Dicer-substrate siRNA molecules were obtained from Integrated DNA Technologies (IDT, Coralville, IA). The sense and antisense sequences of a previously developed siRNA against exon 1 of AR mRNA (siARNTD) were 5'-ccAuGcAACUCcUuCaGcAACAGdcda-3' and 5'-UGcUGUUGcUgAaGGAGUUGCAuGgug-3'.^[35] A siLuc was used as a negative control (sense, 5'-cuuAcGcuGAGuAcuucGAdTsdT-3'; antisense, 5'-UCGAAGuACuACGGuAAGdTsdT-3').^[17] Lower case letters indicate 2'-O-methyl modification and "s" indicates phosphorothioate linkages between the 3'-deoxythymidine overhangs.

Production of Lipid Nanoparticles Containing siRNA and Lipophilic Taxane Prodrugs: LNPs containing siRNA and lipophilic prodrugs were prepared by rapid mixing through a T-junction mixer as previously described.^[27,31,32,39] Briefly, DLin-MC3-DMA, DSPC, cholesterol, PEG-DMG or PEG-DSG, and lipophilic prodrugs were dissolved in ethanol at appropriate ratios (Table S1, Supporting Information) to a final concentration of $10 \times 10^{-3}\text{ M}$ total lipid (TL). Nucleic acids were dissolved in $25 \times 10^{-3}\text{ M}$ sodium acetate buffer at pH 4.0 to obtain a final mixture with a defined nucleic acid to lipid weight/ μmol ratio of 0.0278 (N/P 6). The organic and aqueous solutions were mixed at a flow ratio of 1:3 (v:v) and a total flow rate of 28 mL min^{-1} . The resulting mixtures were dialyzed against a 1000-fold volume of phosphate-buffered saline (PBS) pH 7.4 overnight and sterile filtered ($0.2\ \mu\text{m}$).

Physicochemical Analysis of Lipid Nanoparticles: Particle size was determined by dynamic light scattering and zeta potential by laser Doppler electrophoresis (LDE) using a Malvern Zetasizer NanoZS (Malvern Instruments, Worcestershire, UK). Lipid concentrations were determined by measuring the cholesterol content of the LNPs (Cholesterol E Assay, Wako Chemicals, Richmond, VA) or their phospholipid content (Phospholipids C Assay, Wako Chemicals). The Quant-iT RiboGreen RNA Assay was used to determine siRNA encapsulation and concentration in LNPs according to manufacturer's protocols (ThermoFisher, Waltham, MA). LNP morphology was visualized by cryoTEM as previously described.^[40] In short, 2–5 μL of concentrated LNPs ($20\text{--}25\text{ mg mL}^{-1}$ total lipid) was added to Lacey-formvar copper grids, and plunge-frozen using an FEI Mark IV Vitrobot (FEI, Hillsboro, OR). Grids were stored in liquid nitrogen until imaged. Grids were moved into a Gatan transfer station pre-equilibrated to at least $-180\text{ }^\circ\text{C}$ prior to add grids to the cryogenic grid holder. An FEI LaB6 G2 TEM (FEI, Hillsboro, OR) operating at 200 kV under low-dose conditions was used to image all samples. A bottom-mount FEI Eagle 4K CCD camera was used to capture all images at a 47–55 000 \times magnification with a nominal underfocus of 1–2 μm to enhance contrast. Sample preparation and imaging were performed at the University of British Columbia Bioimaging Facility (Vancouver, BC).

In Vitro Degradation of Prodrugs: To determine prodrug biodegradability, 1 mg mL⁻¹ of LNPs containing siLuc and 10 mol% docetaxel prodrugs LD18 or LD22 was incubated in CD1 mouse plasma (Cedarlane, Burlington, ON) for 24 h at 37 °C. Post incubation, four volumes of chloroform/methanol (2:1) were added and vortex-mixed. Samples were centrifuged at 13 000 × g for 5 min and the upper phase was discarded. The remaining organic phase was dried down under vacuum, and the resulting lipid extract was dissolved in methanol/isopropanol (1:1). Quantity of parent taxane prodrug was determined by ultra-high-performance liquid chromatography (UPLC) on a Waters Acquity H-Class UPLC System equipped with a BEH C18 column (1.7 μm, 2.1 × 100 mm) and a photodiode array detector. Separation was achieved at a flow rate of 0.5 mL min⁻¹, with a linear gradient of mobile phases A:B from 30:70 to 100:0 (v:v) over 3 min followed by an isocratic hold at 100:0 for an additional 3 min. Column temperature was maintained at 55 °C. Mobile phase A consisted of equal parts of methanol and acetonitrile, while mobile phase B was water. The absorbance at 230 nm was measured, and the analyte concentration was determined using calibration curves.

Cell Lines: The human prostate cancer cell lines 22Rv1 (CRL-2505), LNCaP clone FGC (CRL-1740), PC3 (CRL-1435), and VCaP (CRL-2876) were obtained from the American Type Culture Collection (Manassas, VA). 22Rv1 and LNCaP cells were maintained in RPMI-1640 medium supplemented with 10% (v:v) fetal bovine serum (FBS). PC3 and VCaP cells were maintained in Dulbecco's modified Eagle medium (DMEM) supplemented with 10% FBS. All cell lines were kept in culture at 37 °C in a humidified atmosphere containing 5% CO₂. Cell culture medium and reagents were obtained from Gibco (ThermoFisher Scientific, Valencia, CA). Cells were propagated to a maximum of 20 passages.

In Vitro Gene-Silencing Experiments: Cells were seeded at 100 000–200 000 cells per well in a 6-well plate and left to adhere overnight in culture medium. The following day, medium was replaced with regular culture medium containing LNP-siRNA at a dose corresponding to 0.05 or 0.1 μg mL⁻¹ siRNA. After 24 or 48 h incubation, medium was aspirated, and cells were washed three times with cold PBS followed by addition of lysis buffer. Cellular mRNA levels of β-actin and AR-V7 were determined as previously described.^[35] Briefly, cellular RNA was isolated using an Invitrogen PureLink RNA Mini Kit (ThermoFisher Scientific) and used as template to synthesize complementary DNA (cDNA) using a High-Capacity cDNA Reverse Transcription Kit (Applied Biosystems, Foster City, CA). qPCR was performed using the synthesized cDNA template, TaqMan Fast Advanced Master Mix (Applied Biosystems), and primer-probe assays (IDT) on a Step One Plus Real-Time PCR System (Applied Biosystems). The AR-V7 primer-probe assay included primer 1, 5'-TTGTCCATCTTGTCTTCG-3'; primer 2, 5'-CAATTGCCAACCCGGAATTT-3'; and probe, 5'-TGAAGCAGGGATGACTCTGGGAGA-3'. The β-actin primer-probe assay, used as a housekeeping gene for standardizing AR-V7 gene expression levels, included: primer 1, 5'-CCTTGCACATGCCGGAG-3'; primer 2, 5'-ACAGAGCCTCGCCTTTG-3'; and probe, 5'-TCATCCATGGTGGCTGGCGG-3'. Gene probes had a double-quenched design, comprising a 5' carboxyfluorescein (FAM) fluorophore, an internal ZEN (IDT) quencher, and a 3' Iowa Black fluorescent quencher (IBFQ) quencher. For relative gene expression, AR-V7 mRNA levels were normalized to β-actin mRNA levels using the delta cycle threshold (ΔC_T) method and the following formula: 2^{-ΔC_T} where ΔC_T = AR-V7 C_T - β-actin C_T.

Cell Viability Experiments: The therapeutic effect of free taxane (pro)drugs and LNP formulations was determined by the [3-(4,5-dimethylthiazol-2-yl)-5-(3-carboxymethoxyphenyl)-2-(4-sulfophenyl)-2H-tetrazolium (MTS)-based CellTiter 96 AQueous One Solution Cell Proliferation Assay (Promega) or the resazurin-based PrestoBlue assay (ThermoFisher). For both assays, 10 000–15 000 cells per well (22Rv1, LNCaP, and VCaP) or 1500 cells per well (PC3) were seeded in 96-well plates and left to adhere overnight in regular culture medium. The following day, medium was aspirated and replaced with regular culture medium containing increasing concentrations of taxane (pro)drugs or LNP formulations. After 72 or 96 h, medium containing treatment was aspirated and replaced by medium containing MTS or

PrestoBlue solution. Following 0.5–4 h incubation at 37 °C, absorbance was measured at 490 nm (MTS) or fluorescence at 530/570 nm (PrestoBlue). Percentage of cell viability was determined by comparing to untreated and dimethyl sulfoxide (DMSO) controls.

Pharmacokinetic and Biodistribution Studies in Mice: 6–8 weeks old female CD1 mice (Charles River Laboratories, Wilmington) were injected intravenously with radiolabeled LNP-siRNA containing ¹⁴C-DSPC or ³H-CHE and 10 mol% (³H-radiolabeled) lipophilic docetaxel prodrugs LD18 or LD22, corresponding to a dose of 2.5 or 4 mg kg⁻¹ siRNA and ≈17 or ≈30 mg kg⁻¹ prodrug. At various time points post injection, mice were anesthetized intraperitoneally with a terminal dose of ketamine-xylazine prior to blood sample collection in ethylenediaminetetraacetic acid (EDTA) tubes via cardiac puncture. Animals were subsequently euthanized by cervical dislocation followed by tissue collection. Tissues were homogenized in PBS using Fastprep tubes and a Fastprep-24 (MP Biomedical, Santa Ana, CA). Tissue homogenates and blood were subsequently subjected to a digestion and decolorization protocol as previously described.^[41] Radioactivity of homogenates, blood samples, and LNPs was measured using a Beckman Coulter LS 6500 liquid scintillation counter (Mississauga, ON, Canada). The percent recovery in blood was calculated based on a blood volume of 70 mL kg⁻¹ body weight.^[41] Blood and tissue radioactivity are expressed as percent injected dose (%ID) or percent injected dose per gram (% ID g⁻¹) of tissue, respectively. All procedures were approved by the Animal Care Committee at the University of British Columbia and were performed in accordance with guidelines established by the Canadian Council on Animal Care.

Biodistribution Study in Tumor-Bearing Mice: 6–10 weeks old male NRG (NOD-Rag1^{null}/L2rg^{null}) mice were inoculated subcutaneously on the right flank with 2 × 10⁶ 22Rv1 cells suspended in 50% Matrigel. Tumor growth was monitored by determining tumor volumes using a digital caliper. The tumor volume V (in mm³) was calculated using the formula V = (π/6)LS² where L is the largest diameter and S is the smallest superficial diameter. When tumors reached a size of ≈250 mm³, mice were injected intravenously with LNP-siRNA containing ¹⁴C-DSPC and 10 mol% ³H-radiolabeled docetaxel prodrugs LD18 or LD22, corresponding to a dose of 5 mg kg⁻¹ siRNA and ≈30 mg kg⁻¹ lipophilic prodrug. At 24 h post injection, mice were anesthetized with CO₂ followed by blood collection in EDTA tubes via cardiac puncture. Plasma was separated from whole blood by centrifugation for analysis. Animals were subsequently euthanized followed by tissue and tumor collection. To determine radioactivity, tissue homogenates and plasma were processed as described in the previous section. Plasma and tissue radioactivity are expressed as % ID or % ID g⁻¹ of tissue, respectively. To determine AR mRNA levels in tumors, total RNA was isolated from tumor homogenates using the TRIzol (Invitrogen) protocol according to the manufacturer's instructions as previously described.^[35] Tumor mRNA levels of β-actin, AR, and AR-V7 were determined as described in the In Vitro Gene-Silencing Experiments Section. All procedures were approved by the Animal Care Committee at the University of British Columbia and BC Cancer Agency and were performed in accordance with guidelines established by the Canadian Council on Animal Care.

Statistical Analysis: Curve fitting and statistical analyses were performed with GraphPad Prism 8 software. Pharmacokinetic parameters were analyzed based on a one compartmental analysis of plasma after intravenous bolus using PKSolver.^[42]

Supporting Information

Supporting Information is available from the Wiley Online Library or from the author.

Acknowledgements

The authors are grateful for the dedicated support of Dr. Nancy Dos Santos and Nicole Wretham (BC Cancer Agency) during studies

with tumor-bearing mice, Dominik Witzigmann (University of British Columbia) for assisting with pharmacokinetic analysis and Joslyn Quick (University of British Columbia) for assisting with tissue processing and RNA analysis. R.v.d.M.'s research on LNPs was supported by funding from the European Union's Horizon 2020 research and innovation program under the Marie Skłodowska-Curie grant agreement No. 660426 and a Veni STW Fellowship (#14385) from the Netherlands Organization for Scientific Research (NWO). The work undertaken by J.Z., J.A.K., and P.R.C. was funded by a Foundation Grant (FDN 148469) from the Canadian Institute for Health Research (CIHR). The work of R.M.S. on LNPs had received funding from the European Union's Horizon 2020 research and innovation program under grant agreement No. 721058.

Conflict of Interest

M.A.C. is a co-founder of Integrated Nanotherapeutics. P.R.C. is a co-founder and shareholder of Acuitas Therapeutics and Precision Nanosystems and Scientific Director and CEO of the NMIN. S.C., J.Z., and Y.Y.C.T. are employees of Integrated Nanotherapeutics. Y.K.T. is an employee of Acuitas Therapeutics.

Author Contributions

R.v.d.M. designed all experiments, formulated all LNPs used throughout the study, performed physicochemical analyses, conducted in vitro and in vivo studies, and wrote the manuscript. S.C. co-designed experiments; assisted with LNP production and analysis, characterization studies, radiolabeled lipophilic prodrug synthesis, tissue collection, and processing; and reviewed the manuscript. J.Z. synthesized DLin-MC3-DMA, PEG lipids, and (radiolabeled) lipophilic taxane prodrugs for all studies, and reviewed the manuscript. J.A.K. assisted with LNP production and analysis, conducted cryoTEM imaging, tissue collection and processing, and reviewed the manuscript. X.R.S.Z. assisted with LNP production and analysis, cell viability experiments, and qPCR studies. Y.K.T. performed injections and tissue collection. M.B.B. co-designed the biodistribution study and reviewed the manuscript. R.M.S. co-designed experiments and co-wrote the manuscript. P.R.C. co-designed experiments and co-wrote the manuscript. Y.Y.C.T. co-designed and supervised all experiments, assisted in tissue collection, and co-wrote the manuscript.

Data Availability Statement

Research data are not shared.

Keywords

androgen receptor, combination treatment, lipid nanoparticles, modularity, platform technology, prodrug, prostate cancer, siRNA

Received: May 24, 2021
Published online: August 1, 2021

- [1] R. L. Setten, J. J. Rossi, S. Han, *Nat. Rev. Drug Discovery* **2019**, *18*, 421.
[2] N. Pardi, M. J. Hogan, F. W. Porter, D. Weissman, *Nat. Rev. Drug Discovery* **2018**, *17*, 261.
[3] D. Wang, P. W. L. Tai, G. Gao, *Nat. Rev. Drug Discovery* **2019**, *18*, 358.
[4] T. C. Roberts, R. Langer, M. J. A. Wood, *Nat. Rev. Drug Discovery* **2020**, *19*, 673.

- [5] S. T. Crooke, B. F. Baker, R. M. Crooke, X. Liang, *Nat. Rev. Drug Discovery* **2021**, *20*, 427.
[6] J. A. Kulkarni, P. R. Cullis, R. van der Meel, *Nucleic Acid Ther.* **2018**, *28*, 146.
[7] D. Witzigmann, J. A. Kulkarni, S. B. Thomson, S. Chen, B. R. Leavitt, P. R. Cullis, R. van Der Meel, *Nat. Nanotechnol.* **2021**, *16*, 630.
[8] D. Adams, A. Gonzalez-Duarte, W. D. O'Riordan, C. C. Yang, M. Ueda, A. V. Kristen, I. Tournev, H. H. Schmidt, T. Coelho, J. L. Berk, K. P. Lin, G. Vita, S. Attarian, V. Planté-Bordeneuve, M. M. Mezei, J. M. Campistol, J. Buades, T. H. Brannagan, B. J. Kim, J. Oh, Y. Parman, Y. Sekijima, P. N. Hawkins, S. D. Solomon, M. Polydefkis, P. J. Dyck, P. J. Gandhi, S. Goyal, J. Chen, A. L. Strahs, S. V. Nochur, M. T. Sweetser, P. P. Garg, A. K. Vaishnav, J. A. Gollob, O. B. Suhr, *N. Engl. J. Med.* **2018**, *379*, 11.
[9] A. Akinc, M. A. Maier, M. Manoharan, K. Fitzgerald, M. Jayaraman, S. Barros, S. Ansell, X. Du, M. J. Hope, T. D. Madden, B. L. Mui, S. C. Semple, Y. K. Tam, M. Ciufolini, D. Witzigmann, J. A. Kulkarni, R. van der Meel, P. R. Cullis, *Nat. Nanotechnol.* **2019**, *14*, 1084.
[10] A. Fire, S. Xu, M. K. Montgomery, S. A. Kostas, S. E. Driver, C. C. Mello, *Nature* **1998**, *391*, 806.
[11] J. A. Kulkarni, D. Witzigmann, S. Chen, P. R. Cullis, R. van der Meel, *Acc. Chem. Res.* **2019**, *52*, 2435.
[12] L. R. Baden, H. M. El Sahly, B. Essink, K. Kotloff, S. Frey, R. Novak, D. Diemert, S. A. Spector, N. Rouphael, C. B. Creech, J. McGgettigan, S. Khetan, N. Segall, J. Solis, A. Brosz, C. Fierro, H. Schwartz, K. Neuzil, L. Corey, P. Gilbert, H. Janes, D. Follmann, M. Marovich, J. Mascola, L. Polakowski, J. Ledgerwood, B. S. Graham, H. Bennett, R. Pajon, C. Knightly, B. Leav, W. Deng, H. Zhou, S. Han, M. Ivarsson, J. Miller, T. Zaks, *N. Engl. J. Med.* **2020**, *384*, 403.
[13] F. P. Polack, S. J. Thomas, N. Kitchin, J. Absalon, A. Gurtman, S. Lockhart, J. L. Perez, G. Pérez Marc, E. D. Moreira, C. Zerbini, R. Bailey, K. A. Swanson, S. Rojchoudhury, K. Koury, P. Li, W. V. Kalina, D. Cooper, R. W. Frenck, L. L. Hammit, Ö. Türeci, H. Nell, A. Schaefer, S. Ünal, D. B. Tresnan, S. Mather, P. R. Dormitzer, U. Şahin, K. U. Jansen, W. C. Gruber, *N. Engl. J. Med.* **2020**, *383*, 2603.
[14] S. C. Semple, A. Akinc, J. Chen, A. P. Sandhu, B. L. Mui, C. K. Cho, D. W. Sah, D. Stebbing, E. J. Crosley, E. Yaworski, I. M. Hafez, J. R. Dorkin, J. Qin, K. Lam, K. G. Rajeev, K. F. Wong, L. B. Jeffs, L. Nechev, M. L. Eisenhardt, M. Jayaraman, M. Kazem, M. A. Maier, M. Srinivasulu, M. J. Weinstein, Q. Chen, R. Alvarez, S. A. Barros, S. De, S. K. Klimuk, T. Borland, V. Kosovrasti, W. L. Cantley, Y. K. Tam, M. Manoharan, M. A. Ciufolini, M. A. Tracy, A. de Foug erolles, I. MacLachlan, P. R. Cullis, T. D. Madden, M. J. Hope, *Nat. Biotechnol.* **2010**, *28*, 172.
[15] M. Jayaraman, S. M. Ansell, B. L. Mui, Y. K. Tam, J. Chen, X. Du, D. Butler, L. Eltepu, S. Matsuda, J. K. Narayanannair, K. G. Rajeev, I. M. Hafez, A. Akinc, M. A. Maier, M. A. Tracy, P. R. Cullis, T. D. Madden, M. Manoharan, M. J. Hope, *Angew. Chem., Int. Ed. Engl.* **2012**, *51*, 8529.
[16] K. Fitzgerald, M. Frank-Kamenetsky, S. Shulga-Morskaya, A. Liebow, B. R. Bettencourt, J. E. Sutherland, R. M. Hutabarat, V. A. Clausen, V. Karsten, J. Cehelsky, S. V. Nochur, V. Kotelianski, J. Horton, T. Mant, J. Chiesa, J. Ritter, M. Munisamy, A. K. Vaishnav, J. A. Gollob, A. Simon, *Lancet* **2014**, *383*, 60.
[17] G. Basha, M. Ordobadi, W. R. Scott, A. Cottle, Y. Liu, H. Wang, P. R. Cullis, *Mol. Ther. – Nucleic Acids* **2016**, *5*, e363.
[18] Y. Yamamoto, P. J. C. Lin, E. Beraldi, F. Zhang, Y. Kawai, J. Leong, H. Katsumi, L. Fazli, R. Fraser, P. R. Cullis, M. E. Gleave, *Clin. Cancer Res.* **2015**, *21*, 4845.
[19] A. Thess, S. Grund, B. L. Mui, M. J. Hope, P. Baumhof, M. Fotin-Mleczek, T. Schlake, *Mol. Ther.* **2015**, *23*, 1456.
[20] N. Pardi, A. J. Secreto, X. Shan, F. Debonera, J. Glover, Y. Yi, H. Muramatsu, H. Ni, B. L. Mui, Y. K. Tam, F. Shaheen, R. G. Collman, K. Karikó, G. A. Danet-Desnoyers, T. D. Madden, M. J. Hope, D. Weissman, *Nat. Commun.* **2017**, *8*, 14630.

- [21] N. Pardi, M. J. Hogan, R. S. Pelc, H. Muramatsu, H. Andersen, C. R. DeMaso, K. A. Dowd, L. L. Sutherland, R. M. Searce, R. Parks, W. Wagner, A. Granados, J. Greenhouse, M. Walker, E. Willis, J. S. Yu, C. E. McGee, G. D. Sempowski, B. L. Mui, Y. K. Tam, Y. J. Huang, D. Vanlandingham, V. M. Holmes, H. Balachandran, S. Sahu, M. Lifton, S. Higgs, S. E. Hensley, T. D. Madden, M. J. Hope, K. Kariko, S. Santra, B. S. Graham, M. G. Lewis, T. C. Pierson, B. F. Haynes, D. Weissman, *Nature* **2017**, *543*, 248.
- [22] N. Pardi, K. Parkhouse, E. Kirkpatrick, M. McMahon, S. J. Zost, B. L. Mui, Y. K. Tam, K. Karikó, C. J. Barbosa, T. D. Madden, M. J. Hope, F. Krammer, S. E. Hensley, D. Weissman, *Nat. Commun.* **2018**, *9*, 3361.
- [23] J. D. Finn, A. R. Smith, M. C. Patel, L. Shaw, M. R. Youniss, J. van Heteren, T. Dirstine, C. Ciullo, R. Lescaubeau, J. Seitzer, R. R. Shah, A. Shah, D. Ling, J. Growe, M. Pink, E. Rohde, K. M. Wood, W. E. Salomon, W. F. Harrington, C. Dombrowski, W. R. Strapps, Y. Chang, D. V. Morrissey, *Cell Rep.* **2018**, *22*, 2227.
- [24] R. van der Meel, E. Sulheim, Y. Shi, F. Kiessling, W. J. M. M. Mulder, T. Lammers, *Nat. Nanotechnol.* **2019**, *14*, 1007.
- [25] Y. Zhao, F. Fay, S. Hak, J. Manuel Perez-Aguilar, B. L. Sanchez-Gaytan, B. Goode, R. Duivenvoorden, C. de Lange Davies, A. Bjorkoy, H. Weinstein, Z. A. Fayad, C. Perez-Medina, W. J. Mulder, *Nat. Commun.* **2016**, *7*, 11221.
- [26] H. Wang, Z. Lu, L. Wang, T. Guo, J. Wu, J. Wan, L. Zhou, H. Li, Z. Li, D. Jiang, P. Song, H. Xie, L. Zhou, X. Xu, S. Zheng, *Cancer Res.* **2017**, *77*, 6963.
- [27] S. Chen, J. Zaifman, J. A. Kulkarni, I. V. Zhigaltsev, Y. K. Tam, M. A. Ciufolini, Y. Y. C. Tam, P. R. Cullis, *J. Controlled Release* **2018**, *286*, 46.
- [28] M. A. Ciufolini, P. R. Cullis, Y. Y. C. Tam, J. Zaifman, *WO2017106957A1*, **2017**.
- [29] R. Walther, J. Rautio, A. N. Zelikin, *Adv. Drug Delivery Rev.* **2017**, *118*, 65.
- [30] J. Rautio, N. A. Meanwell, L. Di, M. J. Hageman, *Nat. Rev. Drug Discovery* **2018**, *17*, 559.
- [31] J. A. Kulkarni, M. M. Darjuan, J. E. Mercer, S. Chen, R. van der Meel, J. L. Thewalt, Y. Y. C. Tam, P. R. Cullis, *ACS Nano* **2018**, *12*, 4787.
- [32] L. B. Jeffs, L. R. Palmer, E. G. Ambegia, C. Giesbrecht, S. Ewanick, I. MacLachlan, *Pharm. Res.* **2005**, *22*, 362.
- [33] M. Shim, Y. Kim, Y. Park, H. Ahn, *Sci. Rep.* **2019**, *9*, 16794.
- [34] J. B. Lee, K. Zhang, Y. Y. C. Tam, J. Quick, Y. K. Tam, P. J. Lin, S. Chen, Y. Liu, J. K. Nair, I. Zlatev, K. G. Rajeev, M. Manoharan, P. S. Rennie, P. R. Cullis, *Mol. Ther. – Nucleic Acids* **2016**, *5*, e348.
- [35] J. Quick, *M.Sc. Thesis*, University of British Columbia, Vancouver, BC, Canada **2019**.
- [36] S. C. Semple, A. Chonn, P. R. Cullis, *Biochemistry* **1996**, *35*, 2521.
- [37] S. Wilhelm, A. J. Tavares, Q. Dai, S. Ohta, J. Audet, H. F. Dvorak, W. C. W. Chan, *Nat. Rev. Mater.* **2016**, *1*, 16014.
- [38] A. Akinc, A. Zumbuehl, M. Goldberg, E. S. Leshchiner, V. Busini, N. Hossain, S. A. Bacallado, D. N. Nguyen, J. Fuller, R. Alvarez, A. Borodovsky, T. Borland, R. Constien, A. de F ougerolles, J. R. Dorkin, K. N. Jayaprakash, M. Jayaraman, M. John, V. Koteliensky, M. Manoharan, L. Nechev, J. Qin, T. Racie, D. Raitcheva, K. G. Rajeev, D. W. Y. Y. Sah, J. Soutschek, I. Toudjarska, H.-P. P. Vornlocher, T. S. Zimmermann, R. Langer, D. G. Anderson, *Nat. Biotechnol.* **2008**, *26*, 561.
- [39] S. Hirota, C. T. De Ilarduya, L. G. Barron, F. C. Szoka, *BioTechniques* **1999**, *27*, 286.
- [40] J. A. Kulkarni, D. Witzigmann, J. Leung, R. van der Meel, J. Zaifman, M. M. Darjuan, H. M. Grisch-Chan, B. Thöny, Y. Y. C. Tam, P. R. Cullis, *Nanoscale* **2019**, *11*, 9023.
- [41] B. L. Mui, Y. K. Tam, M. Jayaraman, S. M. Ansell, X. Du, Y. Y. C. Tam, P. J. Lin, S. Chen, J. K. Narayanannair, K. G. Rajeev, M. Manoharan, A. Akinc, M. A. Maier, P. Cullis, T. D. Madden, M. J. Hope, *Mol. Ther. – Nucleic Acids* **2013**, *2*, e139.
- [42] Y. Zhang, M. Huo, J. Zhou, S. Xie, *Comput. Methods Prog. Biomed.* **2010**, *99*, 306.